

Shortcuts for causal discovery of nonlinear models by score matching

Francesco Montagna¹, Lorenzo Rosasco^{1,2,3}, Nicoletta Noceti¹, Francesco Locatello⁴

¹MaLGa, Università di Genova

²MIT, CBMM

³Istituto Italiano di Tecnologia (IIT)

⁴Institute of Science and Technology Austria (ISTA)

Abstract

The use of simulated data in the field of causal discovery is ubiquitous due to the scarcity of annotated real data. Recently, Reisach et al. (2021) highlighted the emergence of patterns in simulated linear data, which displays increasing marginal variance in the causal direction. As an ablation in their experiments, Montagna et al. (2023a) found that similar patterns may emerge in nonlinear models for the variance of the score vector $\nabla \log p_{\mathbf{X}}$, and introduced the ScoreSort algorithm. In this work, we formally define and characterize this *score-sortability* pattern of nonlinear additive noise models. We find that it defines a class of identifiable (bivariate) causal models overlapping with nonlinear additive noise models. We theoretically demonstrate the advantages of ScoreSort in terms of statistical efficiency compared to prior state-of-the-art score matching-based methods and empirically show the score-sortability of the most common synthetic benchmarks in the literature. Our findings remark (1) the lack of diversity in the data as an important limitation in the evaluation of nonlinear causal discovery approaches, (2) the importance of thoroughly testing different settings within a problem class, and (3) the importance of analyzing statistical properties in causal discovery, where research is often limited to defining identifiability conditions of the model.

experimenter to actively intervene in the system. This inference problem is commonly known in the literature as *causal discovery*. Summary information about causal relationships between the model variables is often represented in the form of directed acyclic graphs (DAGs) whose nodes are the variables of interest, and edges mark the existence of cause-effect relationships. Traditional causal discovery methods in the constraint and score-based literature are PC (Spirtes et al., 2000) and GES (Chickering, 2003): in the absence of restrictive assumptions on the causal model of the data generating process, these are limited to consistent inference of the Markov equivalence class of the causal graph, where some edges are left undirected, meaning that these methods are often not able to capture the asymmetry between cause and effect. Recently, it has been shown that restrictions on the class of functions generating effects from their causes ensure the *identifiability* of the true DAG (Shimizu et al., 2006; Hoyer et al., 2008; Peters et al., 2014b; Zhang and Hyvärinen, 2009). These theoretical findings have drawn interest in defining algorithms for the inference of the causal graph underlying observational data (Shimizu et al., 2011; Peters et al., 2014a; Bühlmann et al., 2014). In the case of nonlinear additive noise models, a recent branch of the literature has investigated the connection between the score function $\nabla \log p(\mathbf{X})$ of the random vector \mathbf{X} and its underlying causal model. In particular, the SCORE, DAS, and NoGAM algorithms (Rolland et al., 2022; Montagna et al., 2023b,c) define conditions for the identification of the causal order and the edges of a causal graph by score matching estimation of the score function.

Development and evaluation of causal discovery methodologies are significantly affected by the scarce availability of real data. As a consequence, researchers and practitioners tend to rely on synthetic data, which are the *de facto* standard for the evaluation of novel methods. Recently, Reisach et al. (2021) and Reisach et al. (2023) brought to the attention the emergence of patterns in synthetic data generated according to causal models with linear functional mechanisms, which can be exploited to define simple heuristic algorithms achieving state-of-the-art performance on causal discovery. For example, they show that correct estimation of the causal order

1 Introduction

The task of causal reasoning, framed as the ability to predict the effect of active interventions on a system, is central to virtually all scientific domains (Koller and Friedman, 2009; Pearl, 2009; Peters et al., 2017). Frequently, manipulating the variables being investigated can be costly, challenging, or entirely unfeasible. This situation has spurred a growing interest in algorithms that identify causal relationships between measurables from purely observational data without needing the

can be obtained by sorting variables by ascending order of their marginal variance in the case of observations generated through a linear causal model. Their work highlights the limitations of using synthetic data that strictly comply with some model specifications as the only resource for the evaluation of causal discovery methods, whereas it leaves as an open question under which condition assumptions compatible with the identified shortcuts in the data should be considered realistic. In their recent paper, Montagna et al. (2023a) conjectures the emergence of *score-sortability*, a pattern in the variance of the score $\nabla \log p(\mathbf{X})$ of observations generated according to nonlinear additive noise models (ANMs), that tends to increase in the anti-causal direction. In our work, we formally define and extensively investigate the score-sortability of nonlinear additive noise models from an empirical and theoretical perspective. We show that score-sortability defines a new class of identifiable causal models and that it can be exploited to attain state-of-the-art inference accuracy on synthetic datasets generated according to parameters commonly found in the literature, generally improving the statistical efficiency of SCORE, a causal discovery method based on the connection between the score function and the causal graph. Our contributions are summarized as follows:

- We identify a pattern in the score function of data generated according to nonlinear ANM, showing that the variance of the score vector $\nabla \log p(\mathbf{X})$ increases in the anti-causal direction. This is the first work that focuses on the detailed study of patterns emerging in the setting of nonlinear data, whereas Reisach et al. (2021) and Reisach et al. (2023) focus on linear models.
- We empirically show that the most common synthetic datasets for the evaluation of algorithms for nonlinear causal discovery are score-sortable. We regard this lack of diversity in the evaluation data as an important limitation in the literature.
- We demonstrate the state-of-the-art empirical performance of the *ScoreSort* algorithm proposed in Montagna et al. (2023a), which finds the causal order of a graph by iterative identification of leaf nodes as the entries of the score vector where the variance is minimized.
- We define the necessary conditions for the identifiability of the causal order of a bivariate graph from observational data with *ScoreSort*. This defines a new class of identifiable causal models with partial overlap with the class of nonlinear ANM.
- We analyze the statistical properties of *ScoreSort* inference on score-sortable models, showing that it exhibits sample efficiency better than SCORE (Rolland et al., 2022) under suitable assumptions.

2 Background and motivations

In this section, we introduce the problem of causal discovery and the formalism of Structural Causal Models (SCMs).

Then, we provide an overview of recent literature connecting the score function (i.e. the gradient of the log-likelihood of the data) and the causal graph under the assumptions of the nonlinear additive noise model (Hoyer et al., 2008).

2.1 Problem definition

A Structural Causal Model \mathcal{M} is defined by the tuple $(\mathbf{X}, \mathbf{U}, \mathcal{F}, p_{\mathbf{U}})$. This consists of the vector $\mathbf{X} \in \mathbb{R}^d$ of *endogenous* random variables, vertices of the causal graph $\mathcal{G} = (\mathbf{X}, \mathcal{E})$ with the set of edges \mathcal{E} that we want to identify. The vector of the *exogenous* random disturbances $\mathbf{U} \in \mathbb{R}^d$, with the noise terms jointly distributed according to $p_{\mathbf{U}}$. The set of causal mechanisms $\mathcal{F} = (f_1, \dots, f_d)$, deterministic maps assigning values to X_1, \dots, X_d respectively, given their causes and the corresponding error term U_i . Each variable X_i is then defined by a structural equation:

$$X_i := f_i(\text{PA}_i, U_i), \forall i = 1, \dots, d, \quad (1)$$

where $\text{PA}_i \subset \mathbf{X}$ is the set of parents of X_i in the directed and acyclic causal graph \mathcal{G} , and denotes the set of direct causes of X_i . The recursive application of equation 1 induces a joint distribution $p_{\mathbf{X}}$, such that the Markov factorization holds:

$$p_{\mathbf{X}}(\mathbf{X}) = \prod_{i=1}^d p_i(X_i | \text{PA}_i). \quad (2)$$

Causal discovery aims to infer the DAG \mathcal{G} given a collection of n observations drawn from the probability distribution $p_{\mathbf{X}}$. From an algorithmic perspective, one common strategy is to separate the inference task into two steps, the first identifying the topological ordering between the nodes and the second finding the graph’s edges admitted by such causal ordering.

Topological order of a graph. Given a directed acyclic graph $\mathcal{G} = (\mathbf{X}, \mathcal{E})$, one can define a partial ordering of the nodes $\pi = \{\pi_1, \dots, \pi_d\}, \pi_i \in \{1, \dots, d\}$, such that whenever we have $X_i \rightarrow X_j \in \mathcal{E}$, then $i \prec_{\pi} j$ (j is a *successor* of i in the ordering π) (Koller and Friedman, 2009). The permutation π is known as the *topological order* of \mathcal{G} , and allows to disambiguate the direction of the edges in the graph. This is crucial in the context of causal models, as knowledge of the topological order intrinsically distinguishes the cause from the effect between a pair of connected nodes.

Identifiability of the causal graph. Without further restrictions on the SCM of equation 1, it is not possible to infer the topological order of the causal graph from observational data, in which case we say that the model is not *identifiable* (Peters et al., 2017). Instead, observations can inform about the Markov Equivalence Class (MEC) of the graph: given two DAGs, they belong to the same Markov equivalence class if they share the skeleton and the set of *v-structures* (see Definition 6.24 in Peters et al. (2017)). The MEC can be represented as a CPDAG (Complete Partial DAG), where the direction of edges between two variables is often not specified. As a clarifying example, consider the pair of bivariate DAGs $X \rightarrow Y$

and $X \leftarrow Y$: given that they share the same skeleton, they belong to a unique MEC, represented by the undirected graph $X - Y$, where the asymmetry between cause and effect is not specified. In order to identify the topological order of a graph from observational data (i.e. in order to distinguish causes from effects), restrictions on the distribution of the noise terms p_U and on the class of functional mechanisms \mathcal{F} are required.

2.2 Nonlinear Additive Noise Model

Identifiability of the causal structure can be guaranteed under the assumptions of a nonlinear additive noise model (Hoyer et al., 2008; Peters et al., 2014b), which defines the process generating causes from effects as a nonlinear deterministic function with additive noise terms. In particular, the ANM is defined by equation 1 when the following holds:

$$X_i := f_i(\text{PA}_i) + U_i, \forall i = 1, \dots, d, \quad (3)$$

with f_i nonlinear. Additional technical conditions on the class \mathcal{F} of mechanisms and on the joint distribution of the noise terms are sufficient to ensure the identifiability of the model (see Condition 19 in Peters et al. (2014b)).

2.3 The interplay between score matching and causal discovery

Recent works in the literature have proven that it is possible to derive constraints on the gradient of the log-likelihood $\nabla \log p(\mathbf{X})$ (known as the score function) to identify both the topological order and the set of edges of a causal graph under the nonlinear additive noise model. Rolland et al. (2022), Montagna et al. (2023b), and Montagna et al. (2023c) exploits score matching (Hyvärinen, 2005) to define a consistent estimator of the causal graph from observational data. The intuition is that, under identifiable conditions, it is possible to map a probability distribution $p_{\mathbf{X}}$ uniquely to the SCM generating the data. By application of the logarithm to the joint distribution $p_{\mathbf{X}}$, the product in the Markov factorization of equation 2 decomposes into a summation:

$$\log p(\mathbf{X}) = \sum_{i=1}^d \log p_i(X_i | \text{PA}_i).$$

The score function is defined as the gradient of the log-likelihood. In the case of an additive noise model, for each node X_i in the graph the corresponding entry in the score vector is $s_i(\mathbf{X}) := \partial_{X_i} \log p_{\mathbf{X}}(\mathbf{X})$, which equals to:

$$s_i(\mathbf{X}) = \partial_{X_i} \log p_i(X_i | \text{PA}_i) + \sum_{k \in \text{CH}_i} \partial_{X_i} \log p_k(X_k | \text{PA}_k), \quad (4)$$

where CH_i denotes the set of direct children of the node X_i . It is indeed important to notice that the summation takes place over the set of children: in the case of a *leaf* X_l , i.e. a node

with the set of children $\text{CH}_l = \emptyset$, the corresponding component of the score $s_l(\mathbf{X})$ simplifies as follows:

$$s_l(\mathbf{X}) := \partial_{X_l} \log p_{\mathbf{X}}(\mathbf{X}) = \partial_{X_l} \log p_l(X_l | \text{PA}_l). \quad (5)$$

Notice that for nonlinear ANMs the summation over children vanishes if and only if the partial derivative of $\log p_{\mathbf{X}}(\mathbf{X})$ is relative to a leaf node. Intuitively, being able to capture this asymmetry between the entries of the score allows to infer the topological order of a causal graph from the data: Rolland et al. (2022) defines the conditions for the identifiability of the causal direction of nonlinear ANM with Gaussian noise terms by deriving constraints on the score function, whereas Montagna et al. (2023c) generalizes their results on arbitrary ANM without restrictions on the distribution of the noise random variables. The resulting SCORE and NoGAM algorithms (described in detail in Appendix A) provide consistent estimators of the topological order via score matching inference of the gradient of the log-likelihood (Hyvärinen, 2005). The score $\nabla \log p_{\mathbf{X}}(\mathbf{X})$ provides rich information about the causal model underlying the distribution, making the graph identifiable from pure observations. In the remainder of the paper, we show that even a simple heuristic to capture the asymmetry between the components of the score may be used to achieve state-of-the-art performance in causal discovery on data generated according to a nonlinear additive noise model.

2.4 A simple baseline for causal order identification

We have discussed how the structure of the score function can be used for the identification of the topological ordering of a nonlinear ANM. In particular, the problem of *identifiability* of causal graphs amounts to finding asymmetries in the joint distribution of cause-effect pairs: being the $\nabla \log p_{\mathbf{X}}(\mathbf{X})$ a transformation of the distribution of the data, we expect the score vector to be informative about the direction of the causal relations. Having these considerations in mind, we observe that the variance of the score vector of an additive noise model cumulates in the anti-causal direction: in the case of a bivariate graph $X \rightarrow Y$, we have indeed that $\text{Var}[s_X(X, Y)] = \text{Var}[\partial_X \log p_X(X)] + \text{Var}[\partial_X \log p_Y(Y)] + C$, where C is a covariance term, whereas $\text{Var}[s_Y(X, Y)] = \text{Var}[\partial_Y \log p_Y(Y)]$. Comparing the two expressions, we get the intuition that the score of a leaf node can be characterized by a smaller variance with respect to the score of a node with children in the graph. In the following example, we show a simple practical case in which the pattern in the variance of the score of a random variable generated according to a nonlinear causal model can be exploited to identify the topological order by a simple heuristic.

Example 1. Let $\mathbf{X} = (X_1, X_2, X_3)$ causally related according to a fully connected graph \mathcal{G} , and assume the following simple SCM, such that closed-form computations are easy to

perform:

$$\begin{aligned} X_1 &:= U_1, \\ X_2 &:= X_1^2 + U_2, \\ X_3 &:= X_1^2 + X_2^2 + U_3, \end{aligned} \quad (6)$$

where the noise terms are mutually independent random variables following a Gaussian distribution $\mathcal{N}(0, 1)$. The resulting entries of the score function are:

$$\begin{aligned} s_1(\mathbf{X}) &= U_1(2U_2 + 2U_3 - 1) \\ s_2(\mathbf{X}) &= U_2(2U_3 - 1) + 2U_1^2U_3 \\ s_3(\mathbf{X}) &= -U_3, \end{aligned}$$

and the vector of the variance of the score's components is $\text{Var}[s(\mathbf{X})] = (9, 13, 1)$ (detailed computations can be found in Appendix C). Thus, we can identify the leaf node X_3 in the graph as the $\text{argmin}_i \text{Var}[s_i(\mathbf{X})]$. Given the topological order of the graph $\pi = (\pi_1, \pi_2, \pi_3)$, we find that the last element in the ordering is $\pi_3 = 3$. In order to find the complete topological ordering, we remove X_3 from the graph and iteratively repeat the procedure on the pruned graph $\tilde{\mathcal{G}}$ whose set of nodes is $\tilde{\mathbf{X}} := (X_1, X_2)$. We obtain that the entries of the score function are $s_1(\tilde{\mathbf{X}}) = U_1(2U_2 - 1)$ and $s_2(\tilde{\mathbf{X}}) = -U_2$, and the vector of the variance is equal to $\text{Var}[s(\tilde{\mathbf{X}})] = (5, 1)$. As for the previous step, we find the index of the leaf node X_2 as the $\text{argmin}_i \text{Var}[s_i(\tilde{\mathbf{X}})]$. Thus we correctly conclude that the topological order of the graph \mathcal{G} is $\pi = (1, 2, 3)$.

Next, our goal is to define formal conditions under which finding minimal variance in the score components can yield a topological order compatible with the causal graph of a non-linear additive noise model.

3 Score-sortability

In the previous section, we discuss a pattern in the score of data generated according to nonlinear ANMs that is informative about the asymmetry in cause-effect relationships. In particular, Example 1 shows that the score entry of a leaf may be characterized by a smaller variance compared to the score associated with a node with children in the graph. In light of this consideration, we formalize a simple condition under which it is possible to identify leaf nodes of a causal graph from the variance of the score function.

Definition 1 (Score-identifiable leaf). Let $\mathbf{X} \in \mathbb{R}^d$ be a random vector defined by a set of structural equations as in 1. Let X_l be a leaf node of the causal graph associated with the SCM. We say that X_l is score-identifiable if $l = \text{argmin}_i \text{Var}[s_i(\mathbf{X})]$.

Example 1 illustrates the case of a causal graph whose leaf nodes are score-identifiable.

Under the assumption of score-identifiable leaves, we can define an iterative procedure that finds the topological order associated with the set of causal variables $\mathbf{X} \in \mathbb{R}^d$. The details of this method are illustrated in the *ScoreSort* Algorithm

1 box, originally proposed in Montagna et al. (2023a). The idea is that at each iteration, a leaf node is identified as the $\text{argmin}_i \text{Var}[s_i(\mathbf{X})]$, and then it is removed from the graph. At the end of the iterating loop, the resulting output of the algorithm is a causal order π^{score} relative to the set of nodes \mathbf{X} . Given a generic distribution $p_{\mathbf{X}}$ that is Markov with respect to the causal graph \mathcal{G} , it is not always the case that *ScoreSort* defines an ordering compatible with the DAG. Thus, we are interested in quantifying the agreement between π^{score} and the graph \mathcal{G} .

Definition 2 (Score-sortability). Let $\mathcal{G} = (\mathbf{X}, \mathcal{E})$ be a directed acyclic graph with set of nodes $\mathbf{X} \in \mathbb{R}^d$ generated according to a structural causal model \mathcal{M} , and with edges $\mathcal{E} = \{(i, j) : X_i \rightarrow X_j\}$. Moreover, let π be the causal order output of Algorithm 1. We define the score-sortability of \mathcal{M} as follows:

$$\nu := 1 - \frac{\sum_{(i,j) \in \mathcal{E}} \mathbb{1}(j \prec_{\pi} i)}{|\mathcal{E}|} \in [0, 1], \quad (7)$$

where $\mathbb{1}$ is indicator function, $|\mathcal{E}|$ is the number of edges in the graph and $j \prec_{\pi} i$ denotes i successor of j in the ordering vector π .

Intuitively, the score-sortability counts the rate of edges in the ground truth DAG that are not admitted by the ordering π found with Algorithm 1: the rate is then subtracted to 1, such that $\nu = 1$ when π is correct with respect to the graph. For example, the score-sortability of the model in Example 1 is $\nu = 1$, which corresponds to an identifiable causal graph. A score-sortability value $\nu = 0.5$ denotes that the output of *ScoreSort* is equivalent to the expected accuracy of a random ordering. Next, we show that score-sortability defines a new class of identifiable causal models.

Algorithm 1 *ScoreSort* (finite sample estimation in the comments), adapted from Montagna et al. (2023a)

```

 $\mathbf{X} \in \mathbb{R}^d, \mathbf{X} \sim p_{\mathbf{X}} \quad // \mathbf{X} \in \mathbb{R}^{n \times d}$ 
 $\pi \leftarrow []$ 
nodes  $\leftarrow [1, \dots, d]$ 
for  $i = 1, \dots, d$  do
     $s(\mathbf{X}) \leftarrow \nabla \log p_{\mathbf{X}}(\mathbf{X}) \quad // \text{score-matching}(\mathbf{X})$ 
     $\lambda \leftarrow \text{argmin} \text{Var}[s(\mathbf{X})] \quad // \text{argmin} \hat{\text{Var}}[\hat{s}(\mathbf{X})]$ 
     $l \leftarrow \text{nodes}[\lambda]$ 
     $\pi \leftarrow [l, \pi]$ 
    Remove  $\lambda$ -th entry from  $\mathbf{X} \quad // \text{Remove } \mathbf{X}[:, \lambda]$ 
    Remove  $l$  from nodes
end for
return  $\pi$ 

```

3.1 ScoreSort identifiability of the bivariate model

We propose sufficient conditions for the identifiability of a bivariate additive noise model of the form $X := U_X$, $Y := f(U_X) + U_Y$, corresponding to the graph $X \rightarrow Y$. It is immediate to see that the model is identifiable by ScoreSort if and only if $\text{Var}[s_X(X, Y)] > \text{Var}[s_Y(X, Y)]$. From equation 4, we can derive the variance of the score components:

$$\begin{aligned} \text{Var}[s_X(X, Y)] &= \text{Var}[\partial_{U_X} f(U_X)] \text{Var}[\partial_{U_Y} \log p(U_Y)] \\ &\quad + \text{Var}[\partial_{U_X} \log p(U_X)] + 2C \end{aligned} \quad (8)$$

$$\text{Var}[s_Y(X, Y)] = \text{Var}[\partial_{U_Y} \log p(U_Y)], \quad (9)$$

where, with an abuse of notation, the different probability distributions p are discerned by their respective arguments. As a shortcut notation, we also define $C := \text{Cov}[\partial_{U_X} \log p(U_X), \partial_{U_X} f(U_X) \partial_{U_Y} \log p(U_Y)]$.

Proposition 1. *Let $X \rightarrow Y$ be the graph associated with a causal model with structural equations $X := U_X$, $Y := f(U_X) + U_Y$. Then:*

$$\nu = 1 \iff \text{Var}[\partial_{U_X} f(U_X)] > 1 - \frac{\text{Var}[\partial_{U_X} \log p(U_X)]}{\text{Var}[\partial_{U_Y} \log p(U_Y)]} - \frac{2C}{\text{Var}[\partial_{U_Y} \log p(U_Y)]}.$$

According to Proposition 1, the bivariate additive noise model is score-sortable and hence identifiable when the variance of $\partial_{U_X} f(U_X)$ is sufficiently large. Note that this is never the case under the hypothesis of linear causal mechanisms. A proof for Proposition 1 is provided in Appendix E.

Remark 1. *Score-sortability is not limited to the case of nonlinear additive noise models, as the structure of the score function of equation 4 holds for generic causal models that satisfy the Markov factorization in equation 2. Hence, score-sortable models define a new class of identifiable SCMs, which includes additive noise models restricted to the case satisfying the condition of Proposition 1.*

3.2 Score-sortability of ANM datasets

In the case when we can not access the distribution $p_{\mathbf{X}}$, but only a finite set of n observations $X \in \mathbb{R}^{n \times d}$, we can not assess the score-sortability of the model directly. In practice, we can exploit the *ScoreSort* algorithm in the finite samples regime (refer to the Algorithm 1 box): instead of computing the score function $s(\mathbf{X})$ directly from the distribution of the data, this is inferred via score matching by the Stein gradient estimator (Li and Turner, 2017) (see Appendix F), which provides a consistent estimator $\hat{s}(\mathbf{X})$ of the score. Thus, the output of the ScoreSort algorithm is a consistent estimator of the score-sortability of the causal model of interest. In the next section, we discuss the statistical efficiency of ScoreSort in comparison to that of the SCORE algorithm.

3.3 Comparing ScoreSort and SCORE statistical efficiency

In practice, the main difference between SCORE and ScoreSort decision rules for leaf node identification is that SCORE relies on the estimation of the Hessian matrix $\nabla^2 \log p(\mathbf{X})$, whereas ScoreSort is based on the inspection of the first order partial derivatives in the gradient of the log-likelihood. The key point for the comparison of the two algorithms' statistical efficiency is that the Hessian estimator defined in SCORE is found by minimizing the error of a regression problem, which requires access to the score vector $\nabla \log p(\mathbf{X})$: given that this is generally unknown, it is replaced by its score matching estimate $\widehat{\nabla \log p(\mathbf{X})}$. Intuitively, errors in $\widehat{\nabla \log p(\mathbf{X})}$ due to the finiteness of the sample propagate in the values inferred for the Hessian matrix $\nabla^2 \log p(\mathbf{X})$. In what follows, we denote $\partial_{x_i} \widehat{\log p(\mathbf{x})}$ as the score matching estimator of the score entry $s_i(\mathbf{x})$ as defined in the ScoreSort algorithm, and $\partial_{x_i}^2 \widehat{\log p(\mathbf{x})}$ as the estimator of the second order partial derivative of the log-likelihood, as defined in SCORE.

Proposition 2. *Let $X \in \mathbb{R}^{n \times d}$ be a sample generated according to a structural causal model as defined in equation 1. Let $\delta_i^{(k)} := |\partial_{x_i} \log p(\mathbf{x}^{(k)}) - \partial_{x_i} \widehat{\log p(\mathbf{x}^{(k)})}|$, where $\mathbf{x}^{(k)} \in \mathbb{R}$ is a row of the matrix X . Let also $\epsilon_i^{(k)} := |\partial_{x_i}^2 \log p(\mathbf{x}^{(k)}) - \partial_{x_i}^2 \widehat{\log p(\mathbf{x}^{(k)})}|$. Assume that if $\partial_{x_i} \widehat{\log p(\mathbf{x}^{(k)})} = \partial_{x_i} \log p(\mathbf{x}^{(k)})$, then $\partial_{x_i}^2 \widehat{\log p(\mathbf{x}^{(k)})} = \partial_{x_i}^2 \log p(\mathbf{x}^{(k)})$. Then,*

$$\epsilon_i^{(k)} = \delta_i^{(k)} \left| \partial_{x_i} \log p(\mathbf{x}^{(k)}) + \partial_{x_i} \widehat{\log p(\mathbf{x}^{(k)})} \right|.$$

Intuitively, the statistical error of first-order partial derivatives propagates in the second-order estimators: as $\left| \partial_{x_i} \log p(\mathbf{x}^{(k)}) + \partial_{x_i} \widehat{\log p(\mathbf{x}^{(k)})} \right|$ gets larger, we expect ScoreSort to display statistical efficiency better than SCORE in the inference of the causal graph. (Proof in Appendix H.)

Remark 2. *To simplify the analysis, Proposition 2 assumes that if the score $\partial_{x_i} \log p(\mathbf{x}^{(k)})$ is exactly known, then the regression error for the second-order estimator also vanishes. In practice, this is not guaranteed, and SCORE may have even larger errors.*

Remark 3. *Proposition 2 highlights the connection between the assumptions of identifiability of a causal model and the statistical error in the inference of the graph. In particular, in score-sortable settings, ScoreSort represents a baseline with statistical efficiency better than SCORE for sufficiently large values of $\left| \partial_{x_i} \log p(\mathbf{x}^{(k)}) + \partial_{x_i} \widehat{\log p(\mathbf{x}^{(k)})} \right|$.*

4 Experimental results

In this section, we investigate ScoreSort's empirical performance, as well as the score-sortability of real and synthetic data commonly used for the evaluation of nonlinear causal discovery algorithms.

Methods. We compare ScoreSort accuracy with order-based methods regarded as state-of-the-art for inference on additive noise models, namely SCORE, NoGAM, CAM (Bühlmann et al., 2014), and RESIT (Peters et al., 2014a) algorithms¹ (see Appendix B).

Metrics. In order to evaluate the score-sortability of a causal model, we use the $\text{FNR}-\hat{\pi}$ accuracy introduced in Montagna et al. (2023a), that measures the false negative rate against the ground truth of the unique fully connected graph compatible with the topological order $\hat{\pi}$. Given a sorting $\hat{\pi}$ inferred from a causal discovery method, the $\text{FNR}-\hat{\pi}$ is defined as the false negative rate of the DAG with edges $\mathcal{E}_{\hat{\pi}} = \{X_{\hat{\pi}_i} \rightarrow X_{\hat{\pi}_j} : \hat{\pi}_i \prec_{\hat{\pi}} \hat{\pi}_j, \forall i, j = 1, \dots, d\}$. In the case of a fully connected graph, a false negative corresponds to an edge with the direction reversed with respect to the target. If $\hat{\pi}$ is correct with respect to the ground truth graph, then $\text{FNR}-\hat{\pi} = 0$. When $\hat{\pi}$ is the order inferred with the ScoreSort algorithm, $\text{FNR}-\hat{\pi}$ evaluates the score-sortability of the causal graph, which can be simply found as $\nu = 1 - \text{FNR}-\hat{\pi}$. Additionally, we use the Structural Hamming Distance (SHD), counting the number of missing and reversed edges in the prediction. The SHD records are reported in Section K of the appendix, as our main goal is the analysis of the score-sortability of the data.

4.1 Score-sortability of synthetic data

The most common strategy for the generation of synthetic causal graphs consists of stochastic sampling of an acyclic graph, randomly generating the causal mechanisms either as a Gaussian process (*GP data*) or via a transformation defined by a neural network (*NN data*) (a thorough list of references where this data simulation setting is employed can be found in Appendix D.2). The standard practice is to generate the causal graphs with the Erdős-Renyi (Erdos and Renyi, 1960) and the Scale-free models (Barabasi and Albert, 1999) (experiments on Scale-free networks are reported in Appendix J). In our experiments, we consider datasets of 1000 samples of sparse and dense graphs with $\{5, 10, 20, 50\}$ nodes (Appendix D.1 for details on the data generation).

GP data experiments. Figure 1 illustrates the empirical results on additive noise model synthetic data with Erdős-Renyi graphs and causal mechanisms sampled from a Gaussian process. We observe that the ScoreSort algorithm performance is comparable to that of SCORE and NoGAM for all combinations of density and graph size while being comparable to or significantly better than CAM and RESIT. Overall, we conclude that *GP data* are score-sortable, given that ScoreSort achieves $1 - \text{FNR}-\hat{\pi}$ (estimate of the data score-sortability) with median in the range $[0.8, 1.0]$.

NN data experiments. Figure 2 shows the empirical results on data simulated from nonlinear ANMs and Erdős-Renyi

	ScoreSort	SCORE	NoGAM	CAM	RESIT
SACHS	0.47	0.47	0.47	0.47	0.35
SynTReN	0.52 \pm 0.1	0.55 \pm 0.13	0.54 \pm 0.11	0.5 \pm 0.16	0.64 \pm 0.12

Table 1: $\text{FNR}-\hat{\pi}$ (the lower, the better) on the SynTReN and Sachs datasets. For SynTReN data, we report mean and standard deviation on 20 random seeds.

graphs, and mechanisms parametrized by neural networks. We see that ScoreSort generally infers the topological order with accuracy consistently better than random, comparable to that of SCORE and NoGAM. We conclude that *NN data* are generally characterized by high score-sortability, given that the median values of the estimated score-sortability are in the range $[0.8, 1.0]$.

Implications. Our experiments demonstrate the score-sortability of the most popular simulated data for the evaluation of nonlinear causal discovery methods, showcasing limitations in the diversity of these common benchmarks. Instead, we advocate for (1) testing the score-sortability of any proposed future benchmark and (2) extending the evaluation of causal discovery methods beyond score-sortable datasets.

4.2 Score-sortability of real data

In this section, we discuss the score-sortability of real and semi-synthetic data. We consider a biological dataset of gene expression records with 17 edges and 853 observations, known as Sachs data (Sachs et al., 2005) (a common benchmark in the causal discovery literature). Additionally, we experiment on 20 distinct semi-synthetic datasets sampled from SynTReN generator of realistic gene expression records (Van den Bulcke et al., 2006), consisting of 1000 samples from a casual graph with 20 nodes and variable number of edges from 19 to 34. In Table 1, we observe that both score-sortability and the benchmarked methods’ performance decrease when compared to experiments on simulated data. Given that real data allow no control over the process generating the observations, these results may be explained by the fact that the model underlying the samples does not comply with the nonlinear ANM and the score-sortable model’s hypothesis.

4.3 Discussion

Our experiments on simulated environments show that the most common synthetic benchmarks for nonlinear causal discovery, with mechanisms sampled from Gaussian processes and random neural networks, consist of *score-sortable* causal models, such that the variance of the score vector can be used to identify the topological order with state-of-the-art performance. This implies that when relying exclusively on *GP* and *NN data* generated according to our parameters, the experiments probe the inference ability of causal discovery methods in the restricted class of score-sortable models. In our Proposition 1 we show that ANMs may not satisfy

¹We consider the DoDiscover implementation of SCORE, NoGAM, CAM (Li et al.), and a custom implementation of RESIT based on the LiNGAM repository.

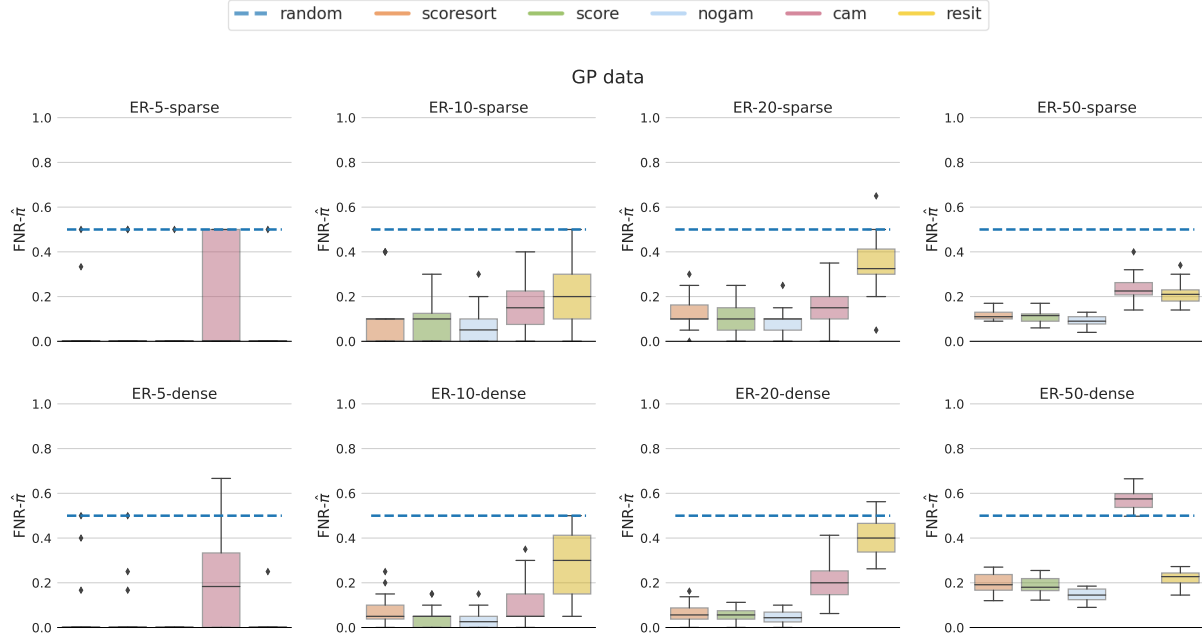


Figure 1: Experimental results on dense and sparse ER with number of nodes in the set $\{5, 10, 20, 50\}$ and GP causal mechanisms. The graphs show the $\text{FNR}-\hat{\pi}$ accuracy (the lower, the better) of the order estimates, with the boxplots evaluated over 20 random seeds. Score-sortability is defined as $\nu = 1 - \text{FNR}-\hat{\pi}$ achieved by ScoreSort, such that low values of $\text{FNR}-\hat{\pi}$ denotes high score-sortability of the model. The dashed blue line is the expected accuracy of random ordering.

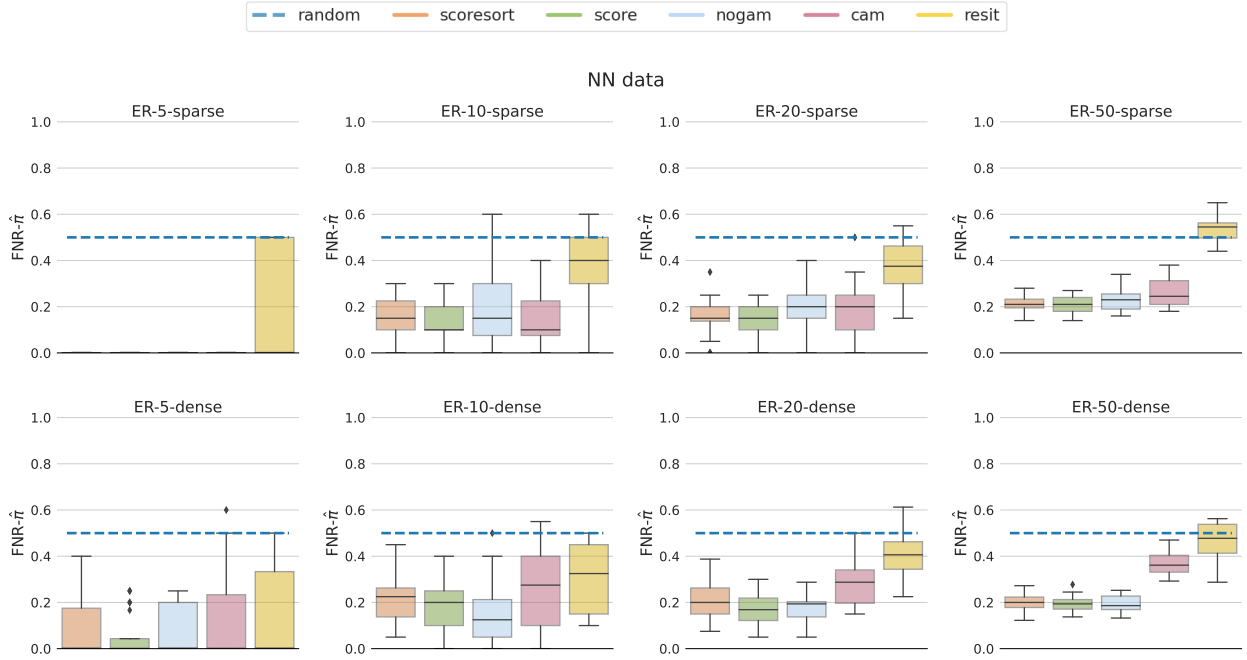


Figure 2: Experimental results on dense and sparse ER with number of nodes in the set $\{5, 10, 20, 50\}$ and NN causal mechanisms. The graphs show the $\text{FNR}-\hat{\pi}$ accuracy (the lower, the better) of the order estimates, with the boxplots evaluated over 20 random seeds. Score-sortability is defined as $\nu = 1 - \text{FNR}-\hat{\pi}$ achieved by ScoreSort, such that low values of $\text{FNR}-\hat{\pi}$ denotes high score-sortability of the model. The dashed blue line is the expected accuracy of random ordering.

score-sortability, while the assumptions for score-sortability do not directly imply the additive noise model (Remark 1): then, empirical evaluation bounded to score-sortable scenarios provides biased information on the performance of methods requiring the ANM hypothesis, restricted to the subclass of inference problems where the simple ScoreSort baseline represents the state of the art. This lack of diversity in the data posits a fundamental limitation in the evaluation of causal discovery approaches for the nonlinear additive noise model: we advise that (1) any future benchmark should assess the score-sortability of the data and (2) that meaningful evaluation should not be limited to score-sortable scenarios.

5 Conclusion

We characterize the score-sortability pattern emerging in data generated by nonlinear causal models, where the variance of the components of the score $\nabla \log p_{\mathbf{X}}(\mathbf{X})$ increases in the anti-causal direction. This property of the data can be exploited for the identification of the causal order: we show that score-sortable causal models are accurately inferred by ScoreSort, which generally improves the statistical efficiency of the SCORE algorithm for ANMs. Our contribution extends to the nonlinear setting the discussion on patterns arising in simulated data presented in Reisach et al. (2021) and Reisach et al. (2023). As one of our key findings, we show that the most common synthetic benchmarks for the evaluation of methods for causal discovery on additive noise models are all characterized by high values of score-sortability. Given that the set of score-sortable models only partially overlaps with ANMs, this implies that the most common evaluation strategies in the literature only provide a biased view of the algorithms’ performance, limited to a subclass of the causal models satisfying the required ANM assumptions. We leave as future work the study of alternative patterns emerging in nonlinear scenarios beyond the restricted case of additive noise models, as well as the characterization of their plausibility in real-world applications.

References

- Albert-Laszlo Barabasi and Reka Albert. Emergence of scaling in random networks. *Science*, 286(5439): 509–512, 1999. doi: 10.1126/science.286.5439.509. URL <http://www.sciencemag.org/cgi/content/abstract/286/5439/509>.
- Philippe Brouillard, Sébastien Lachapelle, Alexandre Lacoste, Simon Lacoste-Julien, and Alexandre Drouin. Differentiable causal discovery from interventional data. In *Proceedings of the 34th International Conference on Neural Information Processing Systems*, NIPS’20, Red Hook, NY, USA, 2020. Curran Associates Inc. ISBN 9781713829546.
- Peter Bühlmann, Jonas Peters, and Jan Ernest. CAM: Causal additive models, high-dimensional order search and penalized regression. *The Annals of Statistics*, 42(6), dec 2014. URL <https://doi.org/10.1214/2F14-aos1260>.
- Tianyu Chen, Kevin Bello, Bryon Aragam, and Pradeep Ravikumar. iscan: Identifying causal mechanism shifts among nonlinear additive noise models, 2023.
- David Maxwell Chickering. Optimal structure identification with greedy search. *J. Mach. Learn. Res.*, 3 (null):507–554, mar 2003. ISSN 1532-4435. doi: 10.1162/153244303321897717. URL <https://doi.org/10.1162/153244303321897717>.
- Paul Erdos and Alfred Renyi. On the evolution of random graphs. *Publ. Math. Inst. Hungary. Acad. Sci.*, 5:17–61, 1960.
- Patrik Hoyer, Dominik Janzing, Joris M Mooij, Jonas Peters, and Bernhard Schölkopf. Nonlinear causal discovery with additive noise models. In D. Koller, D. Schuurmans, Y. Bengio, and L. Bottou, editors, *Advances in Neural Information Processing Systems*, volume 21. Curran Associates, Inc., 2008. URL <https://proceedings.neurips.cc/paper/2008/file/f7664060cc52bc6f3d620bcedc94a4b6-Paper.pdf>.
- Aapo Hyvärinen. Estimation of non-normalized statistical models by score matching. *Journal of Machine Learning Research*, 6(24):695–709, 2005. URL <http://jmlr.org/papers/v6/hyvarinen05a.html>.
- Nan Rosemary Ke, Silvia Chiappa, Jane X Wang, Jorg Bornschein, Anirudh Goyal, Melanie Rey, Theophane Weber, Matthew Botvinick, Michael Curtis Mozer, and Danilo Jimenez Rezende. Learning to induce causal structure. In *International Conference on Learning Representations*, 2023. URL https://openreview.net/forum?id=hp_RwhKDJ5.
- D. Koller and N. Friedman. *Probabilistic Graphical Models: Principles and Techniques*. Adaptive computation and machine learning. MIT Press, 2009. ISBN 9780262013192. URL <https://books.google.co.in/books?id=7dzpHCHzNQ4C>.
- Sébastien Lachapelle, Philippe Brouillard, Tristan Deleu, and Simon Lacoste-Julien. Gradient-based neural dag learning. In *International Conference on Learning Representations*, 2020. URL <https://openreview.net/forum?id=rk1bKA4YDS>.
- Adam Li, Jaron Lee, Francesco Montagna, Chris Trevino, and Robert Ness. Dodiscover: Causal discovery algorithms in Python. URL <https://github.com/py-why/dodiscover>.
- Yingzhen Li and Richard Turner. Gradient estimators for implicit models. 05 2017.
- Phillip Lippe, Taco Cohen, and Efstratios Gavves. Efficient neural causal discovery without acyclicity constraints. In *International Conference on Learning Rep-*

- resentations, 2022. URL <https://openreview.net/forum?id=eYciPrLuUhG>.
- Qiang Liu, Jason Lee, and Michael Jordan. A kernelized stein discrepancy for goodness-of-fit tests. In Maria Florina Balcan and Kilian Q. Weinberger, editors, *Proceedings of The 33rd International Conference on Machine Learning*, volume 48 of *Proceedings of Machine Learning Research*, pages 276–284, New York, New York, USA, 20–22 Jun 2016. PMLR. URL <https://proceedings.mlr.press/v48/liub16.html>.
- Christos Louizos, Uri Shalit, Joris Mooij, David Sontag, Richard Zemel, and Max Welling. Causal effect inference with deep latent-variable models. In *Proceedings of the 31st International Conference on Neural Information Processing Systems, NIPS’17*, page 6449–6459, Red Hook, NY, USA, 2017. Curran Associates Inc. ISBN 9781510860964.
- Francesco Montagna, Atalanti Mastakouri, Elias Eulig, Nicoletta Noceti, Lorenzo Rosasco, Dominik Janzing, Bryon Aragam, and Francesco Locatello. Assumption violations in causal discovery and the robustness of score matching. In *(To appear) Proceedings of the 37th International Conference on Neural Information Processing Systems*, 2023a.
- Francesco Montagna, Nicoletta Noceti, Lorenzo Rosasco, Kun Zhang, and Francesco Locatello. Scalable causal discovery with score matching. In *2nd Conference on Causal Learning and Reasoning*, 2023b. URL <https://openreview.net/forum?id=6VvoDjLBPQV>.
- Francesco Montagna, Nicoletta Noceti, Lorenzo Rosasco, Kun Zhang, and Francesco Locatello. Causal discovery with score matching on additive models with arbitrary noise. In *2nd Conference on Causal Learning and Reasoning*, 2023c. URL <https://openreview.net/forum?id=rV00Bx90deu>.
- RP Monti, K Zhang, and A Hyvärinen. Causal discovery with general non-linear relationships using non-linear ica. 10 2019.
- Joris Mooij, Jonas Peters, Dominik Janzing, Jakob Zscheischler, and Bernhard Schölkopf. Distinguishing cause from effect using observational data: Methods and benchmarks. *Journal of Machine Learning Research*, 17:1–102, 04 2016.
- Joris M Mooij, Dominik Janzing, Tom Heskes, and Bernhard Schölkopf. On causal discovery with cyclic additive noise models. In J. Shawe-Taylor, R. Zemel, P. Bartlett, F. Pereira, and K.Q. Weinberger, editors, *Advances in Neural Information Processing Systems*, volume 24. Curran Associates, Inc., 2011. URL https://proceedings.neurips.cc/paper_files/paper/2011/file/d61e4bbd6393c9111e6526ea173a7c8b-Paper.pdf.
- Judea Pearl. *Causality: Models, Reasoning and Inference*. Cambridge University Press, USA, 2nd edition, 2009. ISBN 052189560X.
- Jonas Peters, Joris M. Mooij, Dominik Janzing, and Bernhard Schölkopf. Causal discovery with continuous additive noise models. *Journal of Machine Learning Research*, 15(58):2009–2053, 2014a. URL <http://jmlr.org/papers/v15/peters14a.html>.
- Jonas Peters, Joris M. Mooij, Dominik Janzing, and Bernhard Schölkopf. Causal discovery with continuous additive noise models. *J. Mach. Learn. Res.*, 15(1):2009–2053, jan 2014b. ISSN 1532-4435.
- Jonas Peters, Dominik Janzing, and Bernhard Schölkopf. *Elements of Causal Inference: Foundations and Learning Algorithms*. The MIT Press, 2017. ISBN 0262037319.
- Alexander Reisach, Christof Seiler, and Sebastian Weichwald. Beware of the simulated dag! varsortability in additive noise models, 02 2021.
- Alexander G. Reisach, Myriam Tami, Christof Seiler, Antoine Chambaz, and Sebastian Weichwald. Simple sorting criteria help find the causal order in additive noise models, 2023.
- Patrik Reizinger, Yash Sharma, Matthias Bethge, Bernhard Schölkopf, Ferenc Huszár, and Wieland Brendel. Jacobian-based causal discovery with nonlinear ICA. *Transactions on Machine Learning Research*, 2023. ISSN 2835-8856. URL <https://openreview.net/forum?id=2Yo9xqR6Ab>.
- Paul Rolland, Volkan Cevher, Matthäus Kleindessner, Chris Russell, Dominik Janzing, Bernhard Schölkopf, and Francesco Locatello. Score matching enables causal discovery of nonlinear additive noise models. In Kamalika Chaudhuri, Stefanie Jegelka, Le Song, Csaba Szepesvari, Gang Niu, and Sivan Sabato, editors, *Proceedings of the 39th International Conference on Machine Learning*, volume 162 of *Proceedings of Machine Learning Research*, pages 18741–18753. PMLR, 17–23 Jul 2022.
- Karen Sachs, Omar Perez, Dana Pe’er, Douglas A. Lauffenburger, and Garry P. Nolan. Causal protein-signaling networks derived from multiparameter single-cell data. *Science*, 308(5721):523–529, 2005. URL <https://www.science.org/doi/abs/10.1126/science.1105809>.
- Shohei Shimizu, Patrik O. Hoyer, Aapo Hyvärinen, and Antti Kerminen. A linear non-gaussian acyclic model for causal discovery. *J. Mach. Learn. Res.*, 7:2003–2030, dec 2006. ISSN 1532-4435.
- Shohei Shimizu, Takanori Inazumi, Yasuhiro Sogawa, Aapo Hyvärinen, Yoshinobu Kawahara, Takashi Washio, Patrik Hoyer, and Kenneth Bollen. Directlingam: A direct method for learning a linear non-gaussian structural equation model. *Journal of Machine Learning Research*, 12, 01 2011.

- P. Spirtes, C. Glymour, and R. Scheines. *Causation, Prediction, and Search*. MIT press, 2nd edition, 2000.
- Charles Stein, Persi Diaconis, Susan Holmes, and Gesine Reinert. Use of exchangeable pairs in the analysis of simulations. *Lecture Notes-Monograph Series*, 46:1–26, 2004. ISSN 07492170. URL <http://www.jstor.org/stable/4356331>.
- Charles M. Stein. A bound for the error in the normal approximation to the distribution of a sum of dependent random variables. 1972.
- Tim Van den Bulcke, Koenraad Leemput, Bart Naudts, Piet Remortel, Hongwu Ma, Alain Verschoren, Bart De Moor, and Kathleen Marchal. Syntren: a generator of synthetic gene expression data for design and analysis of structure learning algorithms. *BMC bioinformatics*, 7:43, 02 2006. doi: 10.1186/1471-2105-7-43.
- Xiaoqiang Wang, Yali Du, Shengyu Zhu, Liangjun Ke, Zhitang Chen, Jianye Hao, and Jun Wang. Ordering-based causal discovery with reinforcement learning. In *International Joint Conference on Artificial Intelligence*, 2021. URL <https://api.semanticscholar.org/CorpusID:234681065>.
- Kun Zhang and Aapo Hyvärinen. On the identifiability of the post-nonlinear causal model. In *Proceedings of the Twenty-Fifth Conference on Uncertainty in Artificial Intelligence*, UAI '09, page 647–655, Arlington, Virginia, USA, 2009. AUAI Press. ISBN 9780974903958.
- Xun Zheng, Bryon Aragam, Pradeep K Ravikumar, and Eric P Xing. Dags with no tears: Continuous optimization for structure learning. In S. Bengio, H. Wallach, H. Larochelle, K. Grauman, N. Cesa-Bianchi, and R. Garnett, editors, *Advances in Neural Information Processing Systems*, volume 31. Curran Associates, Inc., 2018. URL https://proceedings.neurips.cc/paper_files/paper/2018/file/e347c51419ffb23ca3fd5050202f9c3d-Paper.pdf.
- Jingyi Zhu. Hessian estimation via stein’s identity in black-box problems. In Joan Bruna, Jan Hesthaven, and Lenka Zdeborova, editors, *Proceedings of the 2nd Mathematical and Scientific Machine Learning Conference*, volume 145 of *Proceedings of Machine Learning Research*, pages 1161–1178. PMLR, 16–19 Aug 2022. URL <https://proceedings.mlr.press/v145/zhu22c.html>.
- Shengyu Zhu, Ignavier Ng, and Zhitang Chen. Causal discovery with reinforcement learning. In *International Conference on Learning Representations*, 2020. URL <https://openreview.net/pdf?id=S1g2skStPB>.

A Score matching-based causal discovery

In this section, we present an overview of the ideas behind the SCORE and NoGAM algorithms, that exploit score matching estimation of the gradient of the log-likelihood to infer the topological ordering of nonlinear additive noise models.

SCORE. Rolland et al. (2022) defines a formal criterion for the identification of the causal order of a graph underlying an additive noise model with Gaussian distribution of the noise terms. The intuition is that, under these assumptions, the second order partial derivative $\partial_{x_l} s_l(\mathbf{X})$ is a constant if and only if X_l is a leaf.

Lemma 1 (Lemma 1 of Rolland et al. (2022)). *Let \mathbf{X} be a random vector generated according to an identifiable ANM with exogenous noise terms $U_i \sim \mathcal{N}(0, \sigma_i^2)$, and let $X_i \in \mathbf{X}$. Then*

$$\text{Var} [\partial_{x_i} s_i(\mathbf{X})] = 0 \iff X_i \text{ is a leaf, } \forall i = 1, \dots, d. \quad (10)$$

The authors define the SCORE algorithm for the inference of the topological order, given a dataset of i.i.d. observations $X \in \mathbb{R}^{n \times d}$: first, SCORE estimates the diagonal elements of the Jacobian matrix of the score J_s via score matching (using an extension of the Stein gradient estimator proposed by Li and Turner (2017), discussed in its details in Appendix G). Then, it identifies a leaf in the graph as the $\text{argmin}_i \text{Var}[\partial_{x_i} s(\mathbf{X})]$, which is removed from the graph and assigned a position in the order vector. By iteratively repeating this two-steps procedure up to the source nodes, all variables in \mathbf{X} eventually are assigned a position in the causal ordering.

NoGAM. Montagna et al. (2023c) exploits the score function to define a formal criterion for the identification of leaf nodes in a graph induced by an additive noise model without restrictions on the distribution of the noise terms. After some manipulations, it can be shown that the score entry of a leaf X_l defined in equation 5 satisfies

$$s_l(\mathbf{X}) = \partial_{U_l} \log p_l(U_l), \quad (11)$$

such that observations of the pair $(U_l, s_l(\mathbf{X}))$ can be used to learn a predictor of the score entry. For an additive noise model, the authors show that the noise term of a leaf is equal to the residual defined as:

$$R_l := X_l - \mathbf{E}[X_l \mid \mathbf{X} \setminus X_l]. \quad (12)$$

Then, it is possible to find a consistent approximator of the score entry of a leaf node using R_l as the only predictor.

Lemma 2 (Lemma 1 of Montagna et al. (2023c)). *Let \mathbf{X} be a random vector generated according to an identifiable ANM, and let $X_i \in \mathbf{X}$. Then*

$$\mathbf{E} \left[(\mathbf{E}[s_i(\mathbf{X}) \mid R_i] - s_i(\mathbf{X}))^2 \right] = 0 \iff X_i \text{ is a leaf.}$$

Similarly to SCORE, NoGAM algorithm uses score matching estimation to define a procedure for the inference of the topological order by iterative identification of leaf nodes, which are found as the $\text{argmin}_i \mathbf{E} \left[(\mathbf{E}[s_i(\mathbf{X}) \mid R_i] - s_i(\mathbf{X}))^2 \right]$. The residuals $R_i, i = 1, \dots, d$, can be estimated by any regression algorithm.

Once the order is found, both SCORE and NoGAM algorithms select the edges by pruning the fully connected graph compatible with the topological order. This procedure is called *CAM-pruning* and is described in detail in the next section.

B Other methods

Now, we provide details on CAM and RESIT algorithms benchmarked in the experimental section 4.

B.1 CAM

CAM algorithm Bühlmann et al. (2014) infers a causal graph from data generated by an additive Gaussian noise model. First, it infers the topological ordering by finding the permutation of the graph nodes corresponding to the fully connected graph that maximizes the log-likelihood of the data. After inference of the topological ordering, a pruning step is done by variable selection with regression. In particular, for each variable X_j CAM fits a generalized additive model using as covariates all the predecessor of X_j in the ordering, and performs hypothesis testing to select relevant parent variables. This is known as the *CAM-pruning* algorithm. For graphs with size strictly larger than 20 nodes, the authors of CAM propose an additional preliminary edge selection step, known as Preliminary Neighbours Search (PNS): given an order π , variable selection is performed by fitting for each $j = 1, \dots, d$ an additive model of X_j versus all the other variables $\{X_i : X_j \succ X_i \text{ in } \pi\}$, and choosing the K most important predictor variables as possible parents of X_j . This preliminary search step allows scaling CAM pruning to graphs of large dimensions. In our experiments, CAM-pruning is implemented with the preliminary neighbors search only for graphs of size 50, with $K = 20$.

B.2 RESIT

In RESIT (regression with subsequent independence test) Peters et al. (2014b) the authors exploit the independence of the noise terms under causal sufficiency to identify the topological order of the graph. For each variable X_i , they define the residuals $R_i = X_i - \mathbf{E}[X_i | \mathbf{X} \setminus \{X_i\}]$, such that for a leaf node X_l it holds that $R_l = U_l - \mathbf{E}[U_l]$. The method is based on the property that under causal sufficiency, the noise variables are independent of all the preceding variables: after estimating the residuals from the data, it identifies a leaf in the graph by finding the residual R_l that is unconditionally independent of any node $X_i, \forall i \neq l$ in the graph. Once an order is given, they select a subset of the edges admitted by the fully connected graph encoding of the ordering. We implement this final step with CAM-pruning.

C Example 1

In this section, we provide detailed computations of the variance of the score vector relative to Example 1. Given the structural causal model

$$\begin{aligned} X_1 &:= U_1, \\ X_2 &:= X_1^2 + U_2, \\ X_3 &:= X_1^2 + X_2^2 + U_3, \end{aligned} \tag{13}$$

under the assumption of mutually independent noise terms with Gaussian distribution $\mathcal{N}(0, 1)$, according to equation 4 the analytic form of the score components is:

$$-(X_i - f_i(\text{PA}_i)) + \sum_{k \in \text{CH}_i} \partial_{x_i} f_k(\text{PA}_k)(X_k - f_k(\text{PA}_k)).$$

Thus, the score entries for the model of equation 13 are:

$$\begin{aligned} s_1(\mathbf{X}) &= U_1(2U_2 + 2U_3 - 1) \\ s_2(\mathbf{X}) &= U_2(2U_3 - 1) + 2U_1^2 U_3 \\ s_3(\mathbf{X}) &= -U_3. \end{aligned}$$

Now, we proceed with the computation of the marginal variance of the vector components. The variance of $s_1(\mathbf{X})$ is given by:

$$\begin{aligned} \text{Var}[s_1(\mathbf{X})] &= 4\text{Var}[U_1 U_2] + 4\text{Var}[U_1 U_3] + \text{Var}[U_1] \\ &= 4\text{Var}[U_1]\text{Var}[U_2] + 4\text{Var}[U_1]\text{Var}[U_3] + \text{Var}[U_1] \\ &= 4 + 4 + 1 = 9. \end{aligned} \tag{14}$$

It is easy to prove that in equation 14 the covariance terms given by the sum of random variables vanish. For the score entry $s_2(\mathbf{X})$, we get:

$$\begin{aligned} \text{Var}[s_2(\mathbf{X})] &= \text{Var}[U_2(2U_3 - 1) + 2U_1^2 U_3] \\ &= \text{Var}[-U_2 + 2U_2 U_3 + 2U_1^2 U_3] \\ &= \text{Var}[U_2] + 4\text{Var}[U_2 U_3] + 4\text{Var}[U_1^2 U_3] \\ &= 1 + 4\text{Var}[U_2]\text{Var}[U_3] + 4\text{Var}[U_1^2]\text{Var}[U_3] \\ &= 1 + 4 + 8 = 13. \end{aligned}$$

Similarly to the previous case, trivial computations show vanishing covariance. Finally, we can immediately conclude that $\text{Var}[s_3(\mathbf{X})] = \text{Var}[U_3] = 1$, hence the vector of marginal variances of the score is $(9, 13, 1)$. Thus, we correctly Next, we consider the calculation of the marginal variance of the score of the pruned graph $\tilde{\mathcal{G}}$ whose set of nodes is $\tilde{\mathbf{X}} := (X_1, X_2)$. The score components are given by:

$$\begin{aligned} s_1(\tilde{\mathbf{X}}) &= U_1(2U_2 - 1) \\ s_2(\tilde{\mathbf{X}}) &= -U_2. \end{aligned}$$

The marginal variance of the first component is:

$$\begin{aligned} \text{Var}[s_1(\tilde{\mathbf{X}})] &= \text{Var}[U_1(2U_2 - 1)] \\ &= \text{Var}[2U_1 U_2] + \text{Var}[U_1] \\ &= 4\text{Var}[U_1]\text{Var}[U_2] + 1 \\ &= 4 + 1 = 5. \end{aligned}$$

Finally, we have $\text{Var}[s_2(\tilde{\mathbf{X}})] = \text{Var}[U_2] = 1$, such that the vector of marginal variance of the score of $\tilde{\mathbf{X}}$ is $(5, 1)$.

	5 nodes	10 nodes	20 nodes	50 nodes
Sparse	$p = 0.1^*$	$m = 1$	$m = 1$	$m = 2$
Dense	$p = 0.4^*$	$m = 2$	$m = 4$	$m = 8$

* Graphs are re-sampled such that they have at least 2 edges.

Table 2: Density schema for randomly sample graphs. The parameter p denotes the probability of an edge between each pair of nodes in the graph, and m denotes the average number of edges for each node in the graph. We scale the parameter m with the number of nodes, such that the relative density (sparsity) is similar for all graph dimensions.

D Synthetic data

D.1 Additive noise model

In this section, we provide a detailed description of the strategies for the generation of synthetic data under the additive noise model.

Causal graph generation. The simplest model for generation of causal DAG is the Erdős-Renyi (ER) (Erdos and Renyi, 1960), which allows specifying the number of nodes d and the average number of connections per node m (or, alternatively, the probability p of connecting each pair of nodes). In ER graphs, pairs of nodes have the same probability of being connected. Scale-free graphs (SF) are generated under a preferential attachment procedure (Barabasi and Albert, 1999), such that nodes with a higher degree are more likely to be connected with a new node, allowing for the presence of *hubs* (i.e. high degree nodes) in the graphs. Scale-free properties are arguably characteristics of many real-world scenarios (Barabasi and Albert, 1999). In Table 2 we report the schema defining the density of the edges relative to the number of nodes in the graph. Networks generated according to these two models are frequently used for evaluation of the performance of causal discovery algorithms (e.g. Zheng et al. (2018); Montagna et al. (2023b,c,a); Rolland et al. (2022); Lachapelle et al. (2020); Ke et al. (2023)).

Nonlinear causal mechanisms. We consider two common practices for the generation of the nonlinear causal mechanisms of an additive noise model. We sample functions from a Gaussian process, such that $\forall i = 1, \dots, d, f_i(X_{PA_i}) = \mathcal{N}(\mathbf{0}, K(X_{PA_i}, X_{PA_i}))$, a multivariate normal distribution centered at zero and with covariance matrix as the Gaussian kernel $K(X_{PA_i}, X_{PA_i})$, where X_{PA_i} are the observations of the parents of the node X_i . Another common approach is to define nonlinear mechanisms via neural networks, where the mechanism f_i is defined as a multilayer perceptron (MLP) with a single hidden layer of 10 nodes, *leaky ReLU* nonlinear activation, and a normalizing layer. The weights of each network are initialized according to a standard normal distribution. These strategies for nonlinear mechanisms generation are commonly employed in previous works: a thorough list of references is provided in Section D.2 of the appendix.

Additive noise distribution. The additive noise terms U_i are generated as nonlinear transformations $t : \mathbb{R} \rightarrow \mathbb{R}$ of a Gaussian random variable $N_i \sim \mathcal{N}(0, \sigma_i)$, where $\sigma_i \sim U(0.5, 1.0)$ uniformly distributed. In practice, for each node $i = 1, \dots, d$, the corresponding noise term is defined as $U_i := t(N_i)$, where t is parametrized by an MLP with 100 nodes in the single hidden layer, sigmoid activation functions, and weights sampled from $U(-0.5, 0.5)$.

D.2 GP and NN data in the literature

GP and *NN data* defined in this work are one of the most common ways (if not *the* most common) to simulate nonlinear causal mechanisms for data generation, in order to evaluate empirical performance of causal discovery approaches. In what follows, we present a thorough list of papers in the causal discovery literature where nonlinear mechanisms are sampled from a gaussian process or a random neural network, similarly to our *GP* and *NN data*: Mooij et al. (2011); Bühlmann et al. (2014); Peters et al. (2014a); Mooij et al. (2016); Louizos et al. (2017); Monti et al. (2019); Lachapelle et al. (2020); Zhu et al. (2020); Brouillard et al. (2020); Wang et al. (2021); Lippe et al. (2022); Rolland et al. (2022); Montagna et al. (2023a); Chen et al. (2023); Montagna et al. (2023b); Reizinger et al. (2023); Montagna et al. (2023c); Ke et al. (2023).

E Proof of Proposition 1

Proof. Consider the additive noise model $X := U_X, Y := f(U_X) + U_Y$. Given that the possible causal orderings of a bivariate graph are (X, Y) and (Y, X) , showing that $\nu = 1$ is equivalent to proving that $\text{Var}[s_X] > \text{Var}[s_Y]$, where we define $s_X := s_X(X, Y)$ and $s_Y := s_Y(X, Y)$. By equation 8 and equation 9 we can derive the following expression of the score of X :

$$\text{Var}[s_X] = \text{Var}[\partial_{U_X} \log p(U_X)] + \text{Var}[\partial_{U_X} f(U_X)]\text{Var}[s_Y] + 2C, \quad (15)$$

where $C := \text{Cov}[\partial_{U_X} \log p(U_X), \partial_{U_X} f(U_X) \partial_{U_Y} \log p(U_Y)]$.

Then, from equation 15 we can rewrite the variance of s_X as:

$$\text{Var}[s_X] = \text{Var}[s_Y] \left(\text{Var}[\partial_{U_X} f(U_X)] + \frac{\text{Var}[\partial_{U_X} \log p(U_X)]}{\text{Var}[\partial_{U_Y} \log p(U_Y)]} + \frac{2C}{\text{Var}[\partial_{U_Y} \log p(U_Y)]} \right).$$

where, $\text{Var}[s_X]$ is defined as $\text{Var}[s_Y]$ multiplied by a coefficient. Let $\gamma := \left(\text{Var}[\partial_{U_X} f(U_X)] + \frac{\text{Var}[\partial_{U_X} \log p(U_X)]}{\text{Var}[\partial_{U_Y} \log p(U_Y)]} + \frac{2C}{\text{Var}[\partial_{U_Y} \log p(U_Y)]} \right)$: it is immediate to see that for $\gamma > 1$, then $\text{Var}[s_X] > \text{Var}[s_Y]$, and vice-versa, $\gamma \leq 1$ implies $\text{Var}[s_X] \leq \text{Var}[s_Y]$. Hence, we have that

$$\nu = 1 \iff \left(\text{Var}[\partial_{U_X} f(U_X)] + \frac{\text{Var}[\partial_{U_X} \log p(U_X)]}{\text{Var}[\partial_{U_Y} \log p(U_Y)]} + \frac{2C}{\text{Var}[\partial_{U_Y} \log p(U_Y)]} \right) > 1. \quad (16)$$

By further manipulation of equation 16, we obtain:

$$\nu = 1 \iff \text{Var}[\partial_{U_X} f(U_X)] > 1 - \frac{\text{Var}[\partial_{U_X} \log p(U_X)]}{\text{Var}[\partial_{U_Y} \log p(U_Y)]} - \frac{2C}{\text{Var}[\partial_{U_Y} \log p(U_Y)]}.$$

□

F Score matching

The goal of score matching is to infer the score function $s(x) := \nabla \log p(\mathbf{X})$ given an *i.i.d.* sample $X = \{\mathbf{x}^{(k)}\}_{k=1, \dots, n}$, extracted from the density p . In this section, we present a method developed in Li and Turner (2017) for estimating the score at the sample points, i.e., approximating $G := (\nabla \log p(\mathbf{x}^1), \dots, \nabla \log p(\mathbf{x}^n))^T \in \mathbb{R}^{n \times d}$. This resulting *Stein gradient estimator* of the score is the one exploited by the ScoreSort algorithm (Algorithm 1). Our discussion will closely follow that of Section 2.2 of Rolland et al. (2022).

This estimator is based on the Stein identity (Stein, 1972), which states that for any test function $\mathbf{h} : \mathbb{R}^d \rightarrow \mathbb{R}^{d'}$ such that $\lim_{\mathbf{x} \rightarrow \infty} \mathbf{h}(\mathbf{x})p(\mathbf{x}) = 0$, we have

$$\mathbb{E}_p[\mathbf{h}(\mathbf{x}) \nabla \log p(\mathbf{x})^T + \nabla \mathbf{h}(\mathbf{x})] = 0, \quad (17)$$

where $\nabla \mathbf{h}(\mathbf{x}) := (\nabla h_1(\mathbf{x}), \dots, \nabla h_{d'}(\mathbf{x}))^T \in \mathbb{R}^{d' \times d}$.

By approximating the expectation in equation 17 using Monte Carlo, we obtain

$$-\frac{1}{n} \sum_{k=1}^n \mathbf{h}(\mathbf{x}^{(k)}) \nabla \log p(\mathbf{x}^{(k)})^T + \text{err} = \frac{1}{n} \sum_{k=1}^n \nabla \mathbf{h}(\mathbf{x}^{(k)}), \quad (18)$$

where err is a random error term with mean zero, and which vanishes as $n \rightarrow \infty$ almost surely. By denoting $\mathbf{H} = (\mathbf{h}(\mathbf{x}^{(1)}), \dots, \mathbf{h}(\mathbf{x}^{(n)})) \in \mathbb{R}^{d' \times n}$ and $\overline{\nabla \mathbf{h}} = \frac{1}{n} \sum_{k=1}^n \nabla \mathbf{h}(\mathbf{x}^{(k)})$, equation equation 18 reads $-\frac{1}{n} \mathbf{H} \mathbf{G} + \text{err} = \overline{\nabla \mathbf{h}}$. Hence, by using ridge regression, the Stein gradient estimator is defined as:

$$\begin{aligned} \hat{\mathbf{G}}^{\text{Stein}} &:= \arg \min_{\hat{\mathbf{G}}} \|\overline{\nabla \mathbf{h}} + \frac{1}{n} \mathbf{H} \hat{\mathbf{G}}\|_F^2 + \frac{\eta}{n^2} \|\hat{\mathbf{G}}\|_F^2 \\ &= -(\mathbf{K} + \eta \mathbf{I})^{-1} \langle \nabla, \mathbf{K} \rangle, \end{aligned} \quad (19)$$

where $\mathbf{K} := \mathbf{H}^T \mathbf{H}$, $\mathbf{K}_{ij} = \kappa(\mathbf{x}^{(i)}, \mathbf{x}^{(j)}) := \mathbf{h}(\mathbf{x}^{(i)})^T \mathbf{h}(\mathbf{x}^{(j)})$, $\langle \nabla, \mathbf{K} \rangle = n \mathbf{H}^T \overline{\nabla \mathbf{h}}$, $\langle \nabla, \mathbf{K} \rangle_{ij} = \sum_{k=1}^n \nabla_{x_j^k} \kappa(\mathbf{x}^{(i)}, \mathbf{x}^{(k)})$ and $\eta \geq 0$ is a regularisation parameter. One can hence use the kernel trick, and use the estimator equation 19 using any kernel κ satisfying Stein's identity, such as the RBF kernel as shown in Liu et al. (2016).

G Hessian's estimator

Rolland et al. (2022) extends score matching estimation of $\nabla \log p(\mathbf{X})$ by the Stein identity to the inference of the second order matrix of partial derivative $\nabla^2 \log p(\mathbf{X})$, Hessian of the log-likelihood. We propose an overview of the estimation procedure, closely following the discussion in Section 3.2 of Rolland et al. (2022).

First, we need to introduce the second-order Stein identity (Stein et al., 2004; Zhu, 2022). Assuming that the distribution p is twice differentiable, for any $q : \mathbb{R}^d \rightarrow \mathbb{R}$ such that $\lim_{\mathbf{x} \rightarrow \infty} q(\mathbf{x})p(\mathbf{x}) = 0$ and such that $\mathbb{E}[\nabla^2 q(\mathbf{x})]$ exists, the second-order Stein identity states that

$$\mathbb{E}[q(\mathbf{x})p(\mathbf{x})^{-1} \nabla^2 p(\mathbf{x})] = \mathbb{E}[\nabla^2 q(\mathbf{x})], \quad (20)$$

which can be rewritten as

$$\mathbb{E}[q(\mathbf{x}) \nabla^2 \log p(\mathbf{x})] = \mathbb{E}[\nabla^2 q(\mathbf{x}) - q(\mathbf{x}) \nabla \log p(\mathbf{x}) \nabla \log p(\mathbf{x})^T]. \quad (21)$$

In the case of SCORE, in order to identify a leaf of the causal graph we are only interested in estimating the diagonal elements of the score's Jacobian (the Hessian of the log-likelihood) at the sample points, i.e., $J := (\text{diag}(\nabla^2 \log p(\mathbf{x}^{(1)})), \dots, \text{diag}(\nabla^2 \log p(\mathbf{x}^{(n)})))^T \in \mathbb{R}^{n \times d}$. Using the diagonal part of the matrix equation equation 21 for various test functions gathered in $\mathbf{h} : \mathbb{R}^d \rightarrow \mathbb{R}^{d'}$, we can write

$$\mathbb{E}[\mathbf{h}(\mathbf{x})\text{diag}(\nabla^2 \log p(\mathbf{x}))^T] = \mathbb{E}[\nabla_{\text{diag}}^2 \mathbf{h}(\mathbf{x}) - \mathbf{h}(\mathbf{x})\text{diag}((\nabla \log p(\mathbf{x})\nabla \log p(\mathbf{x})^T))],$$

where $(\nabla_{\text{diag}}^2 \mathbf{h}(\mathbf{x}))_{ij} = \frac{\partial^2 h_i(\mathbf{x})}{\partial x_j^2}$. By approximating the expectations by an empirical average, we obtain, similarly as in equation 18,

$$\frac{1}{n} \sum_{k=1}^n \mathbf{h}(\mathbf{x}^{(k)})\text{diag}(\nabla^2 \log p(\mathbf{x}^{(k)}))^T + \text{err} = \frac{1}{n} \sum_{k=1}^n \nabla_{\text{diag}}^2 \mathbf{h}(\mathbf{x}^{(k)}) - \mathbf{h}(\mathbf{x}^{(k)})\text{diag}(\nabla \log p(\mathbf{x}^{(k)})\nabla \log p(\mathbf{x}^{(k)})^T). \quad (22)$$

By denoting $\mathbf{H} = (\mathbf{h}(\mathbf{x}^{(1)}), \dots, \mathbf{h}(\mathbf{x}^{(n)})) \in \mathbb{R}^{d' \times n}$ and $\overline{\nabla_{\text{diag}}^2 \mathbf{h}} := \frac{1}{n} \sum_{k=1}^n \nabla_{\text{diag}}^2 \mathbf{h}(\mathbf{x}^{(k)})$, equation equation 22 reads $\frac{1}{n} \mathbf{H} \mathbf{J} + \text{err} = \overline{\nabla_{\text{diag}}^2 \mathbf{h}} - \frac{1}{n} \mathbf{H} \text{diag}(\mathbf{G} \mathbf{G}^T)$. Hence, by using the Stein gradient estimator for \mathbf{G} , we define the Stein Hessian estimator as the ridge regression solution of the previous equation, i.e.

$$\begin{aligned} \hat{\mathbf{J}}^{\text{Stein}} &:= \arg \min_{\mathbf{J}} \left\| \frac{1}{n} \mathbf{H} \mathbf{J} + \frac{1}{n} \mathbf{H} \text{diag} \left(\hat{\mathbf{G}}^{\text{Stein}} \left(\hat{\mathbf{G}}^{\text{Stein}} \right)^T \right) - \overline{\nabla_{\text{diag}}^2 \mathbf{h}} \right\|_F^2 + \frac{\eta}{n^2} \|\mathbf{J}\|_F^2 \\ &= -\text{diag} \left(\hat{\mathbf{G}}^{\text{Stein}} \left(\hat{\mathbf{G}}^{\text{Stein}} \right)^T \right) + (\mathbf{K} + \eta \mathbf{I})^{-1} \langle \nabla_{\text{diag}}^2, \mathbf{K} \rangle, \end{aligned} \quad (23)$$

where $\mathbf{K}_{ij} = \kappa(\mathbf{x}^{(i)}, \mathbf{x}^{(j)}) := \mathbf{h}(\mathbf{x}^{(i)})^T \mathbf{h}(\mathbf{x}^{(j)})$, $\langle \nabla_{\text{diag}}^2, \mathbf{K} \rangle = n \mathbf{H}^T \overline{\nabla_{\text{diag}}^2 \mathbf{h}}$, $\langle \nabla_{\text{diag}}^2, \mathbf{K} \rangle_{ij} = \sum_{k=1}^n \frac{\partial^2 \kappa(\mathbf{x}^{(i)}, \mathbf{x}^{(k)})}{\partial (x_j^{(k)})^2}$ and $\mathbf{G}^{\text{Stein}}$ is defined in equation 19.

H Proof of Proposition 2

Proof. Let $G := (\nabla \log p(\mathbf{x}^1), \dots, \nabla \log p(\mathbf{x}^n))^T \in \mathbb{R}^{n \times d}$ be the matrix of the score for each observation $\mathbf{x}^{(k)}$ of the sample. Let $\hat{G} := \hat{G}^{\text{stein}}$ defined in equation 19. We define the matrix of the estimation errors as:

$$\begin{aligned} \Delta_G &:= G - \hat{G} \\ &= (\partial_{x_i} \log p(\mathbf{x}^{(k)}) - \partial_{x_i} \log \widehat{p(\mathbf{x}^{(k)})})_{1 \leq k \leq n, 1 \leq i \leq d} \in \mathbb{R}^{n \times d}. \end{aligned} \quad (24)$$

Similarly, we define the estimation error on the diagonal terms of the score's Jacobian. Let $\hat{J}(\hat{G}) := \hat{J}^{\text{stein}}$ defined in equation 23, where the argument \hat{G} is used to remark the dependence from the Stein gradient estimator of equation 19. The resulting matrix of statistical errors is :

$$\begin{aligned} \Delta_{J(\hat{G})} &:= J - \hat{J}(\hat{G}) \\ &= (\partial_{x_i}^2 \log p(\mathbf{x}^{(k)}) - \partial_{x_i}^2 \log \widehat{p(\mathbf{x}^{(k)})})_{1 \leq k \leq n, 1 \leq i \leq d} \in \mathbb{R}^{n \times d}. \end{aligned} \quad (25)$$

Now, consider the case where $\hat{G} = G$, i.e. we have perfect estimates of the score: from equation 23, we have that the score's Jacobian optimal estimator is:

$$\hat{J}(G) := -\text{diag}(GG^T) + (\mathbf{K} + \eta \mathbf{I})^{-1} \langle \nabla_{\text{diag}}^2, \mathbf{K} \rangle, \quad (26)$$

which, by assumption, is subject to zero error, i.e. $J - \hat{J}(G) = 0$.

Remark. We defined the matrix Δ_G of error in the estimation of the score $\nabla \log p(\mathbf{X})$ by using equation 19. Similarly, we define $\Delta_{J(\hat{G})}$ error of estimation when the Hessian of the log-likelihood is computed by equation 23, as a function of \hat{G} . In the case where the matrix G is exactly known, then the statistical error in the inference of J is null by hypothesis.

We want to show that errors in the estimation of G propagate to $\hat{J}(\hat{G})$. We start manipulating the expression of $\hat{J}(\hat{G})$ of equation 23:

$$\begin{aligned} \hat{J}(\hat{G}) &= -\text{diag}(\hat{G} \hat{G}^T) + (\mathbf{K} + \eta \mathbf{I})^{-1} \langle \nabla_{\text{diag}}^2, \mathbf{K} \rangle \\ &= -\text{diag}(\hat{G} \hat{G}^T + G G^T - G G^T) + (\mathbf{K} + \eta \mathbf{I})^{-1} \langle \nabla_{\text{diag}}^2, \mathbf{K} \rangle \\ &= -\text{diag}(G G^T) + (\mathbf{K} + \eta \mathbf{I})^{-1} \langle \nabla_{\text{diag}}^2, \mathbf{K} \rangle + \text{diag}(G G^T - \hat{G} \hat{G}^T) \\ &= \hat{J}(G) + \text{diag}((G - \hat{G})(G + \hat{G})^T) \\ &= \hat{J}(G) + \text{diag}(\Delta_G(G + \hat{G})^T) \end{aligned} \quad (27)$$

Hence, we see that $\hat{J}(\hat{G})$ is equivalent to the ridge regression solution of equation 26, namely the score’s Jacobian estimator computed with the exact value of G , plus an error term that propagates from the first order estimates of the score. Given the assumption $J - \hat{J}(G) = 0$, we get:

$$\begin{aligned} |J - \hat{J}(\hat{G})| &= |J - \hat{J}(G) + \text{diag}(\Delta_G(G + \hat{G})^T)| \\ &= |\Delta_G(G + \hat{G})^T|, \end{aligned}$$

such that for each sample $\mathbf{x}^{(k)}$ in the dataset, the resulting error is defined as:

$$\begin{aligned} \epsilon_i^{(k)} &:= \left| \partial_{x_i}^2 \log p(\mathbf{x}^{(k)}) - \partial_{x_i}^2 \widehat{\log p(\mathbf{x}^{(k)})} \right| \\ &= \left| \partial_{x_i} \log p(\mathbf{x}^{(k)}) - \partial_{x_i} \widehat{\log p(\mathbf{x}^{(k)})} \right| \left| \partial_{x_i} \log p(\mathbf{x}^{(k)}) + \partial_{x_i} \widehat{\log p(\mathbf{x}^{(k)})} \right|. \end{aligned}$$

□

I Other patterns of sortability in the nonlinear additive noise model

In this section, we provide an overview of the *varsortability* and R^2 -*sortability*, two patterns emerging in the setting of linear SCM which can inform about the causal order of the model by simple sorting heuristics.

I.1 Varsortability

Reisach et al. (2021) shows that when the causal mechanisms of the model generating the data are linear, it is possible to identify the topological order of the variable by simple sorting of the variables by ascending order of their variance. In particular, assuming the bivariate causal relation $Y = wX + N_Y$, where w is the linear coefficient of the structural equation, identifiability of the order by the variance of X and Y is verified if and only if $w^2 \text{Var}[X] + \text{Var}[N_Y] > \text{Var}[X]$, which is equivalent to $\text{Var}[Y] > \text{Var}[X]$. Under the hypothesis of a nonlinear causal model $Y = f(X) + N_Y$, the condition on the variance becomes $\text{Var}[f(X)] + \text{Var}[N_Y] > \text{Var}[X]$. The experiments in Reisach et al. (2021) show that *varsortability* is a common feature of simulated additive noise model data, in the case of both linear and nonlinear mechanisms.

I.2 R^2 -sortability.

Closely related to the varsortability of causal models, Reisach et al. (2023) recently identified another pattern emerging in synthetic data generated under the linear model

$$\mathbf{X} = W\mathbf{X} + \mathbf{N},$$

where W denotes the weight matrix and \mathbf{N} is the random vector of the noise terms. The marginal variance of a random variable X_i is defined by $\text{Var}[X_i] = \text{Var}[\mathbf{W}_i]$. Given that varsortability is implied by the increasing marginal variance $\text{Var}[X_i] = \text{Var}[\mathbf{W}_i^T \mathbf{X}] + \text{Var}[N_i]$, with \mathbf{W}_i denoting the i -th row of the matrix W , the intuition is that the variance $\text{Var}[\mathbf{W}_i^T \mathbf{X}]$ explained by the parents of a node also increases in the causal direction. Then, the vector defined by cause-explained variance fraction $(\frac{\text{Var}[\mathbf{W}_i^T \mathbf{X}]}{\text{Var}[X_i]})_i$ may provide information about the causal ordering of the model. Given that the cause-explained variance of a variable can not be directly estimated from the data, the authors of the paper define the coefficient $R_i^2 := 1 - \frac{\text{Var}[X_i - \mathbf{E}[X_i | \mathbf{X} \setminus \{X_i\}]]}{\text{Var}[X_i]}$ as an upper bound of the cause-explained variance, where the expectation $\mathbf{E}[X_i | \mathbf{X} \setminus \{X_i\}]$ can be inferred by regressing X_i on all the remaining nodes in the graph. Then, a model is said to be R^2 -sortable when the causal order is found by sorting the vector of $(R_i^2)_i$ coefficients by their ascending value.

J Experiments on Scale-free graphs

Figure 3 and 4 show the FNR- $\hat{\pi}$ of ScoreSort, SCORE, NoGAM, CAM, and RESIT on sparse and dense Scale-free graphs with $\{10, 20, 50\}$ nodes, and causal mechanisms sampled from Gaussian processes (*GP data*) and random neural networks (*NN data*). We observe that similarly to the case of Erdős-Renyi causal graphs, these common benchmarks tend to be score-sortable. Additionally, we report the Structural Hamming Distance on Scale-free graphs in Figure 5 for *GP data* and Figure 6 for *NN data*.

K Structural hamming distance on Erdős-Renyi graphs

In this section, we report the SHD of the experiments discussed in Section 4 of the main manuscript. Figure 7 shows results for *GP data*, whereas 8 refers to the inference on *NN data*. All the benchmarked methods perform the edge selection step via CAM-pruning procedure (see Appendix B.1), with $\alpha = 0.05$ for the p -value thresholding.

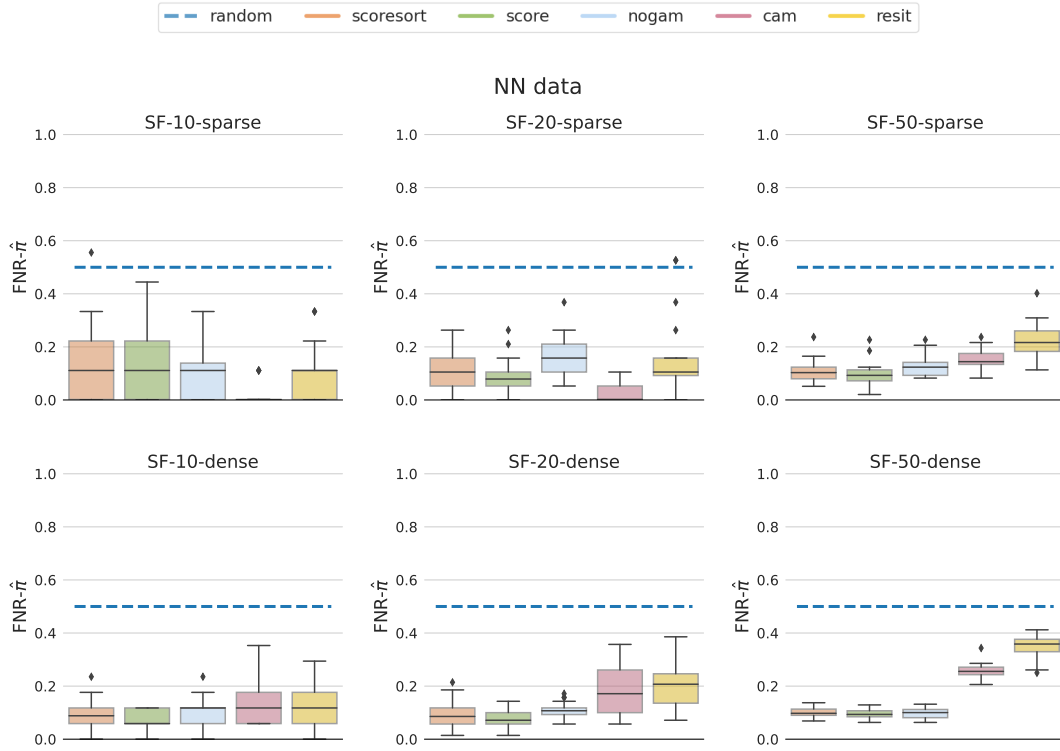


Figure 3: Experimental results on dense and sparse SF with number of nodes in the set $\{10, 20, 50\}$ and GP causal mechanisms. The graphs show the $\text{FNR}-\hat{\pi}$ accuracy (the lower, the better) of the order estimates, with the boxplots evaluated over 20 random seeds. Score-sortability is defined as $\nu = 1 - \text{FNR}-\hat{\pi}$ achieved by ScoreSort, such that low values of $\text{FNR}-\hat{\pi}$ denotes high score-sortability of the model. The dashed blue line is the expected accuracy of random ordering.

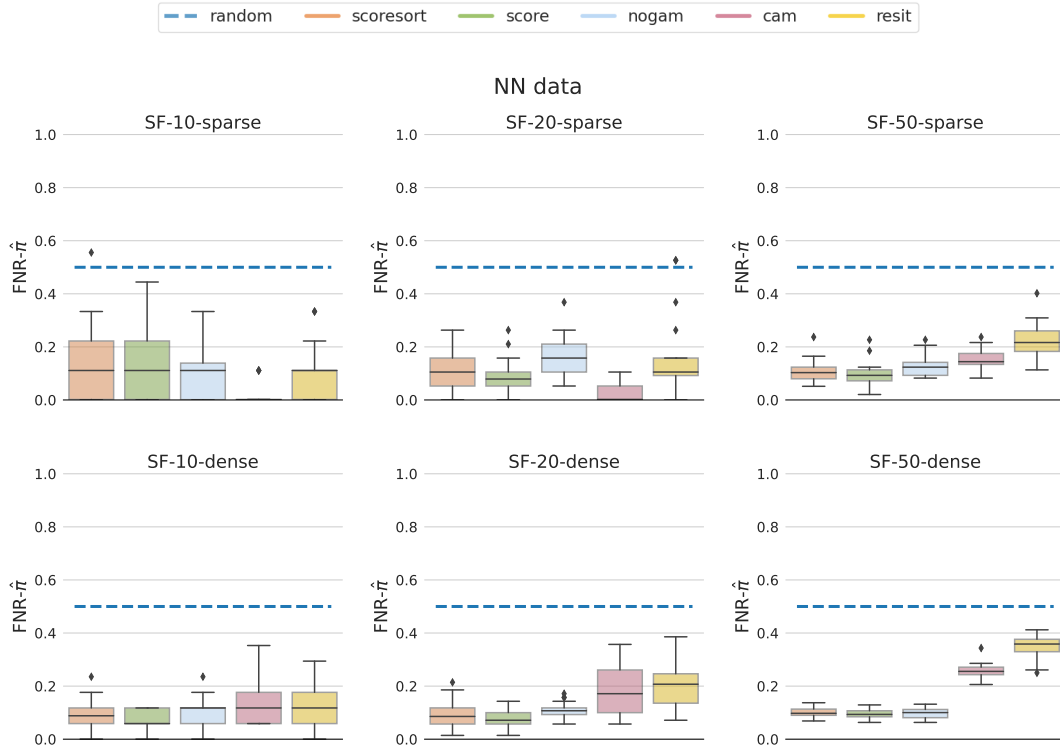


Figure 4: Experimental results on dense and sparse SF with number of nodes in the set $\{10, 20, 50\}$ and NN causal mechanisms. The graphs show the FNR- $\hat{\pi}$ accuracy (the lower, the better) of the order estimates, with the boxplots evaluated over 20 random seeds. Score-sortability is defined as $\nu = 1 - \text{FNR-}\hat{\pi}$ achieved by ScoreSort, such that low values of FNR- $\hat{\pi}$ denotes high score-sortability of the model. The dashed blue line is the expected accuracy of random ordering.

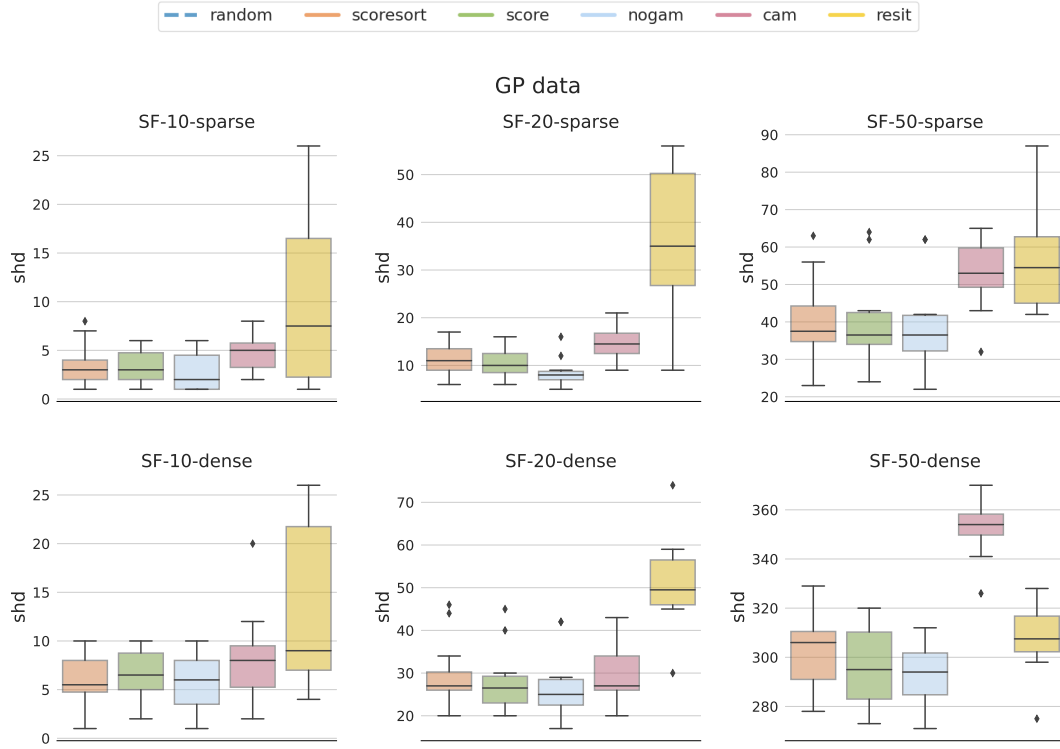


Figure 5: Structural Hamming Distance (the lower, the better) on dense and sparse SF with the number of nodes in the set $\{10, 20, 50\}$ and GP causal mechanisms. Box plots are evaluated over 20 random seeds.

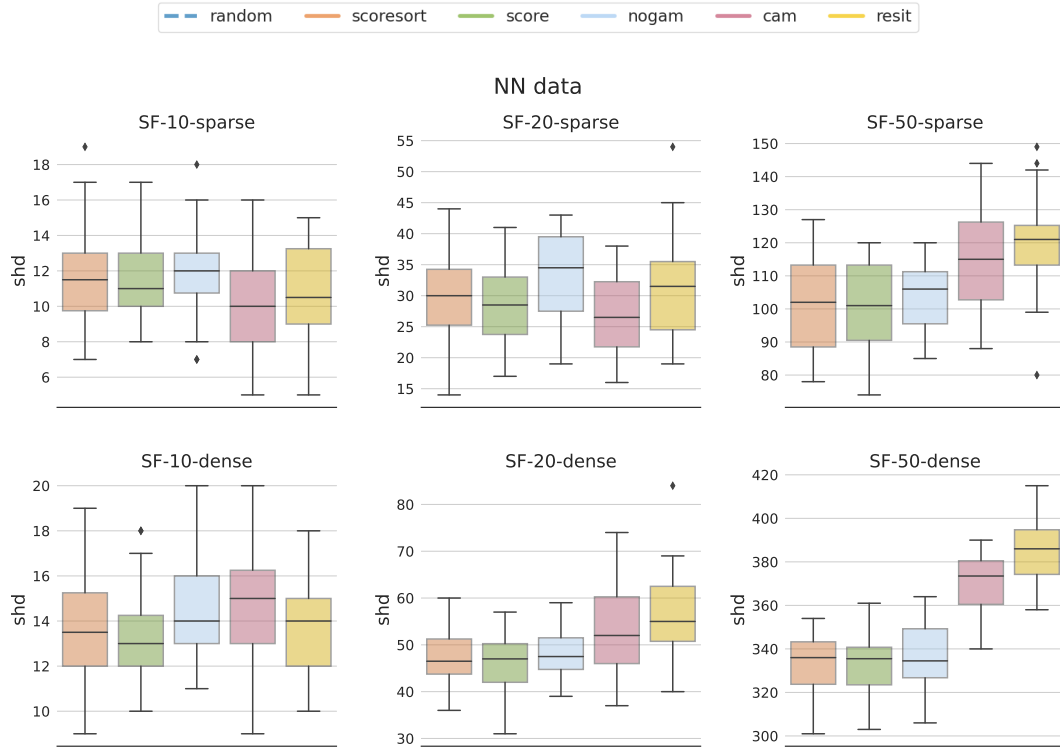


Figure 6: Structural Hamming Distance (the lower, the better) on dense and sparse SF with the number of nodes in the set $\{10, 20, 50\}$ and NN causal mechanisms. Box plots are evaluated over 20 random seeds.

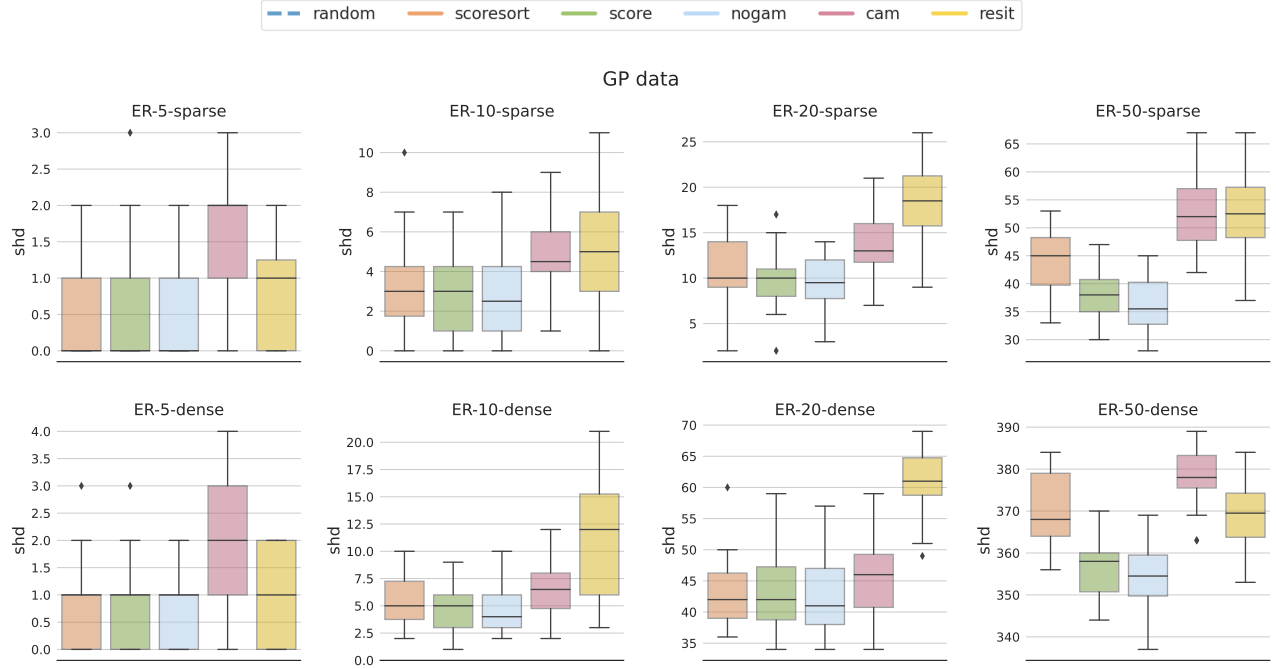


Figure 7: Structural Hamming Distance (the lower, the better) on dense and sparse ER with the number of nodes in the set $\{5, 10, 20, 50\}$ and GP causal mechanisms. Box plots are evaluated over 20 random seeds.

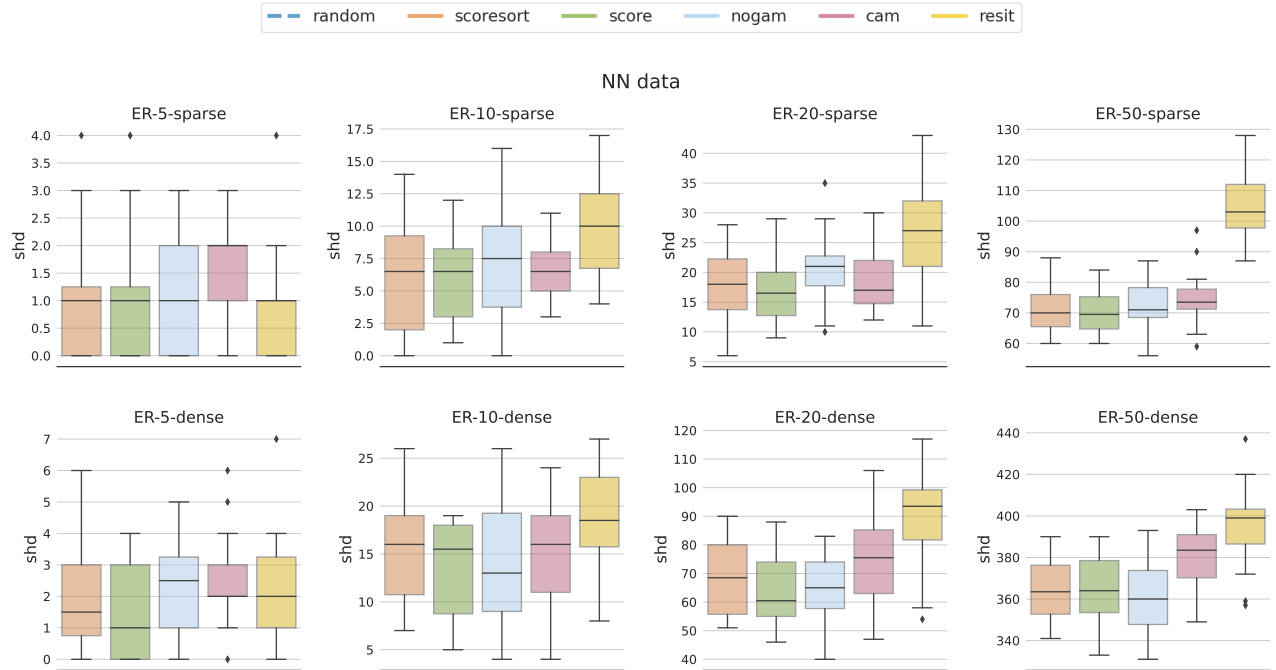


Figure 8: Structural Hamming Distance (the lower, the better) on dense and sparse ER with the number of nodes in the set $\{5, 10, 20, 50\}$ and NN causal mechanisms. Box plots are evaluated over 20 random seeds.